Journal of Mining and Environment (JME) Vol. 15, No. 4, 2024, 1509-1525

Shahrood University of Technology

Journal of Mining and Environment (JME)

Journal homepage: www.jme.shahroodut.ac.ir

Iranian Society of Mining Engineering (IRSME)

Discrete Elements Analysis of Sand Production Mechanism in Oil Well considering Effects of *in-situ* Stress and Fluid Pressure

Masoud Yazdani[1], Mohammad Fatehi Marji[1]*, Hamid Soltanian[2], Mehdi Najafi[1], and Manouchehr Sanei[1]

1. Department of Mining and Metallurgical Engineering, Yazd University, Yazd, Iran
3. Drilling & Well Completion Technologies & Research Group, Research Institution of Petroleum Industry, Tehran, Iran

Article Info

Received 27 November 2023
Received in Revised form 23 December 2024
Accepted 22 January 2024
Published online 22 January 2024

DOI: 10.22044/jme.2024.13894.2585

Keywords

Discrete element method
Sand production
Fluid pressure
Oil well
Modified TWC test

Abstract

Approximately 70% of the world's hydrocarbon fields are located in reservoirs with low-strength rocks such as sandstone. During the production of hydrocarbons from sandstone reservoirs, sand-sized particles may become dislodged from the formation, and enter the hydrocarbon fluid flow. Sand production is a significant issue in the oil industry due to its potential to cause erosion of pipes and valves. Separating grains from oil is a costly process. Therefore, oil and gas-producing companies are motivated to reduce sand production during petroleum extraction. Various methods exist for predicting this phenomenon including continuous, discontinuous, experimental, physical, analytical, and numerical methods. Given the significance of the subject, this research work aims to achieve two primary objectives. Firstly, it proposes a two-dimensional numerical model based on the discrete element method to address the issues of high strain and deformation in granular materials. This method is highly reliable in simulating the mechanism of sand production in oil wells. Secondly, the production of sand is influenced by two factors: fluid pressure and stress; to evaluate changes in production from a particular reservoir, it is necessary to analyze each parameter. Two sandstone samples, similar to reservoir rock conditions, were prepared and tested in the laboratory to demonstrate sand production phenomenon. The numerical results have been verified and compared to their experimental counterparts.

1. Introduction

Sand or solids production is the phenomenon of particle production during the extraction of oil-producing wells. This physical phenomenon occurs when the previously stable fluid/porous medium becomes unstable and reaches the strength limit of the porous matrix, resulting in a breakdown of its constituent parts. [1, 2] indicate that this phenomenon is common. Field observations suggest that perturbations in flow gradients and effective stress acting on the porous matrix of the formation initiate the fracturing of small portions of the rock. Sand production is a common and significant issue encountered during oil or gas extraction. According to the Society of Petroleum Engineers (SPE), a large portion of the world's hydrocarbon reserves are contained in sandstone, and are therefore, susceptible to this phenomenon. Improper control of this problem may render the development of boreholes economically unfeasible or lead to their premature closure. Research [2] estimates that seventy percent of the world's hydrocarbon reserves are contained in reservoirs where sand/solids production may occur. Bianca [3] proposed that the production of sand/solids in oil-producing wells is influenced by three main factors: the magnitude and variation of in-situ stresses, pressure gradients, fluid flow velocity, and changes in fluid saturation; the strength factor (material strength, inter-particle friction, sand arches, and capillary forces); and operational factors (drilling and completion strategies, production procedures, and reservoir depletion). A detailed description of the operational aspects and other mechanisms related to sand/solids production

✉ *Corresponding author: mohammad.fatehi@gmail.com (M. Fatehi Marji)*

can be found in [2, 4]. Recent approaches attempt to predict the rate of sand production. Internal erosion is also a relevant mechanism, as proposed by Papamichos, Vardoulakis, Tronvoll, and Skjirstein (2001), and Papamichos and Vardoulakis (2005). Erosion occurs when the drag force of the fluid is sufficient to overcome the cohesive and frictional strength of the material and carry the particles away [5]. In addition, the fluid can transport finer particles from deeper within the formation. These particles may consist of the original depositional material or may result from particle breakage caused by the increase in effective stress within the formation during the oil recovery process. There is also the possibility of redeposition of the eroded material near the cavity, which can affect stability and flow rate [7, 12, and 20].

Previous studies have highlighted the difficulty in predicting sand production [15, 16]. Furthermore, the numerical modelling of this phenomenon is complex due to the intricate interaction between fluid and solid [21-24]. Despite the development of several numerical models to represent this phenomenon, there is still a fundamental lack of a model to comprehensively present it. The objective of this study is to demonstrate sand production through numerical and experimental methods. A two-dimensional discrete element method (DEM) is employed to solve the problem by considering the granular material with high strain and deformation around the oil well. The effects of fluid pressure and stress on sand production during hydrocarbon extraction are analyzed. A two-dimensional numerical model based on the discrete element method is proposed to simulate the mechanism of sand production for granular materials under high strain and deformation environments. The discrete element method (DEM) is the most reliable method for simulating the mechanism of sand production because it allows for the analysis of the simultaneous effects of fluid pressure and stress, which play a fundamental role in the process. The changes in production from the reservoir can be accurately computed by analysing the changes in each parameter. This research work involved testing two samples of sandstone, similar to those found in real reservoir rock conditions, in a laboratory and simulating them using the two-dimensional particle flow code (PFC2D). The numerical results were compared to the corresponding results obtained from experimental tests, and found to be accurate.

2. Sand Production Mechanisms

Sand production is a process that involves two mechanisms: mechanical instabilities that cause localized plastic behavior and failure of the rock around the cavity, and the subsequent transportation of sand particles due to fluid drag forces. This process is a coupled fluid and solid process [13]. The sandstone rock initially fails close to the cavity, and the failed material is then eroded by the flowing fluid. These two mechanisms are interdependent, as stress concentrations around the eroded cavity result in increased damage. This, in turn, increases the amount of cohesionless material that can be dislodged. The classical approach concentrates on the conditions that trigger sand production, identifying several failure modes, the relevant conditions, and the controlling operational variables [2]. Figure 1 illustrates the three-step process of sand production, which includes near-wellbore damage, perforation, and transportation. Initially, small holes form around the borehole due to sand production. These holes then extend, eventually connecting to form a larger hole, which causes sand to enter the well suddenly [2].

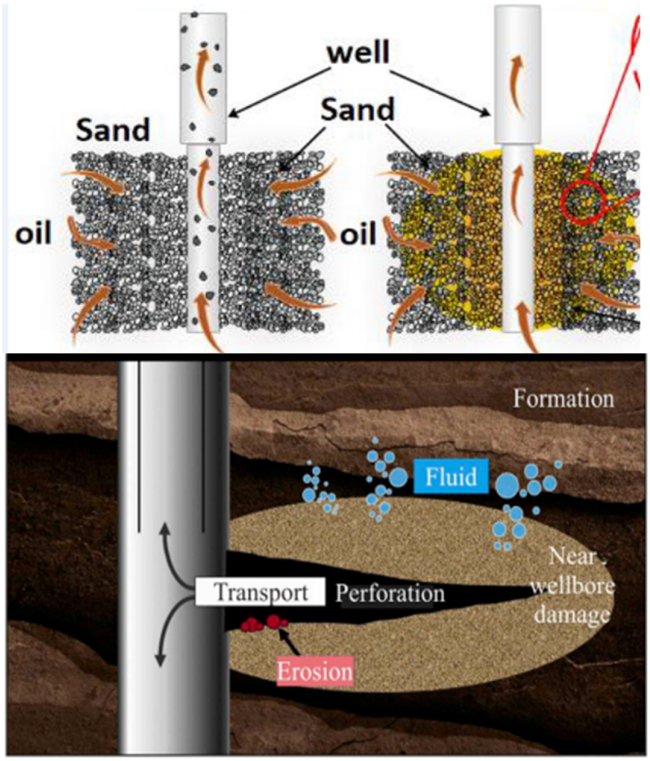

Figure 1. Sand production mechanism [2].

It is important to note that this classification is based on the amount of sand produced in the well over time. To prevent sand production, it is necessary to identify and address the underlying causes. Sand production in wells can be caused by several factors including disturbed stress balance in the layer, movement of fluid, reduction in reservoir pressure, reduction in structure toughness, rock fatigue, and production increase. The amount of sand production is typically classified into three states: unstable, stable, and catastrophic [2].

2.1. Sand production prediction methods

Predicting sand production and its rate is crucial for developing an optimal well completion and exploitation strategy. Various methods are used to predict sand production including analytical, experimental, and numerical methods. These methods are highly complementary, and should be combined to ensure a realistic and consistent approach to predicting sand production.

2.1.1. Theoretical modeling - analytical methods

There are different types of theoretical sand prediction tools depending on the sand failure mechanism considered in the formulation [26]. These mechanisms responsible for sand production are compressive failure, tensile failure, and erosion [34]. Failures and erosion occur near the cavity wall. Shear-compressive failure refers to excessive circumferential stress near the cavity, which causes shear failure of the formation material. Tensile failure is when the tensile radial stress exceeds the tensile failure envelope. Erosion occurs when the drag forces of the fluid flow exceed the apparent cohesion of the particles, and it is a special form of tensile failure. The modeling of compressive failure is highly dependent on the choice of yield envelope and failure criterion [42]. One can choose between yield envelopes such as Drucker-Prager and Mohr-Coulomb, and failure criteria based on maximum plastic strain, maximum plastic zone size or maximum stress. It is necessary to validate the material model against both lab and field sand production data. For instance, linear elastic criteria were used to present equations for sand production and rock fracture around a laboratory well sample [18]. In 2008, improved relationships for this problem were presented by addressing the shortcomings of previous formulas. Additionally, in 2001, Zervos investigated well fracture and stress around the well using three-dimensional movement and presented interesting results from different states of the well site for sand production. The researchers investigated several oil wells, and used mathematical relationships to determine the border between sand and sand production [19]. The

results showed that a shear modulus to bulk ratio greater than 0.8 indicates the beginning of sanding in the well. In 2016, a case study and experiments were conducted using Hook and Brown criteria to determine the volume of sand produced [32]. In 2016, the control of sand production was improved by using complex mathematical relationships and statistical models through the development of the lssvm classification model [20]. While analytical methods are suitable for predicting the onset of sand production [29], they have limitations and are only valid under simplified geometrical and boundary conditions, making them unsuitable for complicated field-scale problems [29].

It is possible to express mathematically the state of the initial and changing stress regimes that affect the strength and stability around the borehole. The stresses around the borehole face play an important role in the response of the rock material to the induced conditions and the associated grinding process. Maximum stress concentrations usually occur near the borehole, particularly at the face of the hole. In linear poroelasticity with no fluid flow and constant pore pressure, the maximum stress is tangential (σθ), and the difference between stresses is greatest at the wellbore opening [32, 43]. Therefore, wellbore failure, and hence sand production, is expected to start at the opening. Since the failure of the rock material near the wellbore is determined by the prevailing stress state, it is necessary to compare the stresses generated with the rock strength using one or more rock failure criteria. In general, the stress solution at the face of a deviated well (Figure 2) is given in cylindrical coordinates as [43]. The parameters in Figure 2 are explained.

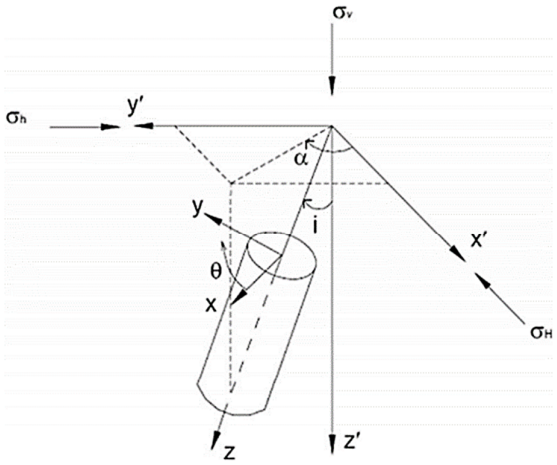

σ_z = Axial stress in (cylindrical coordinates);
σ_θ = Tangential stress (cylindrical coordinates);
σ_r = Radial stress (cylindrical coordinates);
$\tau_{\theta z}, \tau_{r\theta}, \tau_{rz}$ = Shear stresses at the wellbore face;
$\sigma_x^0, \sigma_y^0, \sigma_z^0$ = In situ normal stresses in the x, y, z coordinate system;
$\tau_{xy}^0, \tau_{yz}^0, \tau_{xz}^0$ = In situ shear stresses in the x, y, z coordinate system;
$\sigma_z, \sigma_H, \sigma_h$ = Vertical and horizontal in situ stresses;
υ = Poisson ratio;
η = Poroelastic stress coefficient;
P_w = Wellbore pressure;
P_0 = Pore pressure at the wellbore;
P_f = Pore pressure at far field region;
θ = Angle of rotation about the z axis referenced from the x axis;
α = Biot's coefficient;
φ = Angle of rotation about the z′ axis referenced from the x′ axis;
i = Angle of rotation about the y′ axis referenced from the z′ axis.

Figure 2. Coordinate system transformation for a deviated wellbore [43].

$$\sigma_z = \sigma_z^0 - v[2(\sigma_x^0 - \sigma_y^0)\cos 2\theta + 4\tau_{xy}^0 \sin 2\theta] + 2\vartheta(P_0 - P_f) \quad (1)$$

$$\sigma_\theta = \sigma_x^0 + \sigma_y^0 - 2(\sigma_x^0 - \sigma_y^0)\cos 2\theta - 4\tau_{xy}^0 \sin 2\theta - P_w + 2\vartheta(P_0 - P_f) \quad (2)$$

$$\sigma_r = P_w \quad (3)$$

$$\tau_{\theta z} = 2(-\tau_{xz}^0 \sin\theta + \tau_{yz}^0 \cos\theta) \quad (4)$$

$$\tau_{r\theta} = 0 \quad (5)$$

$$\tau_{rz} = 0 \quad (6)$$

$$\vartheta = \alpha[\frac{1-2v}{2(1-v)}] \quad (7)$$

$$\sigma_z^0 = (\sigma_H \cos^2\varphi + \sigma_h \sin^2\varphi)\sin^2 i + \sigma_v \cos^2 i \quad (8)$$

$$\sigma_x^0 = (\sigma_H \cos^2\varphi + \sigma_h \sin^2\varphi)\cos^2 i + \sigma_v \sin^2 i \quad (9)$$

$$\sigma_y^0 = (\sigma_H \sin^2\varphi + \sigma_h \cos^2\varphi) \quad (10)$$

$$\tau_{xy}^0 = 0.5(\sigma_h - \sigma_H)\, sin2\,\varphi\, cos\, i \quad (11)$$

$$\tau_{yz}^0 = 0.5(\sigma_h - \sigma_H)\, sin2\,\varphi\, sin\, i \quad (12)$$

$$\tau_{xz}^0 = 0.5(\sigma_H \cos^2\varphi + \sigma_h \sin^2\varphi)\, sin2\, i \quad (13)$$

2.1.2. Laboratory experiments

Measurement of produced sand is a crucial aspect of sand production testing. Various methods have been employed for this purpose including discontinuous and continuous measurement using sonic and acoustic instruments as well as measurement with different scales. The results of each test are primarily presented in a graph format, which displays the amount of sand production during the test and under different stress levels and fluid injection conditions. Figure 3 shows an example of these diagrams. They provide information on indicative stress levels such as the stress level at which sand production begins or the stress level at which mass sand production occurs. Several laboratory studies have investigated the impact of grain size and permeability, as well as the effect of two adjacent wells [40, 41].

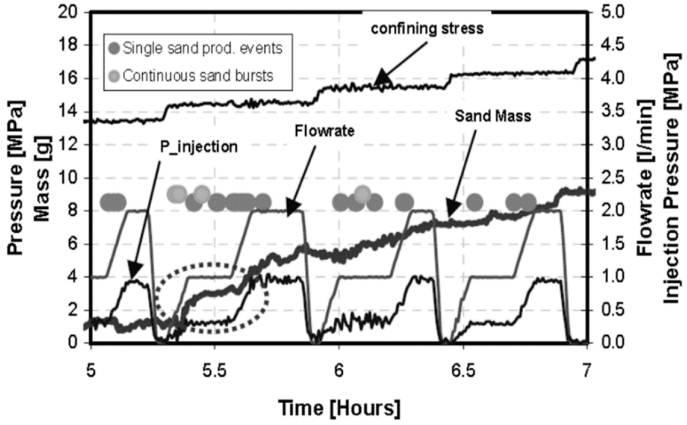

Figure 3. Graph showing the rate of sand production over time during laboratory testing [40].

In-situ testing can be challenging due to the high costs associated with testing at reservoir depth. To observe and simulate sand production in a controlled environment, many researchers conduct laboratory sand production experiments using modified Thick-Walled Cylinder (TWC) tests [34]. These tests provide insights into sand production mechanisms and the influence of various field and operational parameters on sand production. Figure 4 shows schematic examples of modified TWC tests. The samples have an outer diameter of up to 100 mm, which is larger than the usual TWC tests, and an inner cavity size of about 20-25 mm. In some tests, fluid flow is introduced into the sample to study its impact [44, 45].

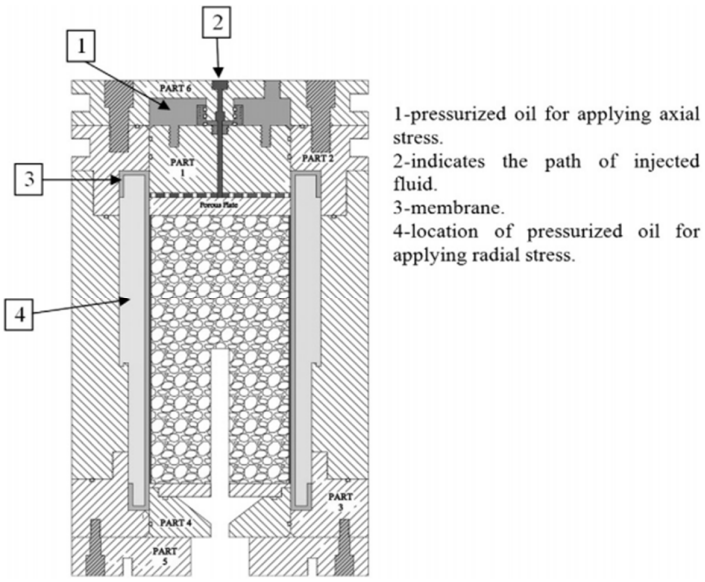

Figure 4. A cross-section of the thick-walled cylinder-shaped device to measure sand production [36, 37].

2.1.3. Numerical methods

Sophisticated and modern numerical methods such as finite element, boundary element, and finite difference methods have been developed for analyzing engineering problems including sand production mechanisms in the oil industry [46, 47, and 48]. Numerical models can be classified as continuum or discrete methods. Most continuum methods are formulated within the framework of the poroelastic theory [4, 15], with plasticity criteria embedded at the limit of elasticity. The fundamental assumption underlying numerical methods is that the materials in question are continuous throughout the physical process. This assumption of continuity implies that the material cannot be broken or separated into distinct pieces at any point in the problem domain. Continuum methods may predict the onset of sand production using mechanical yielding as an indicator, but they struggle to capture micro-cracking and grain movement after the solid matrix disintegrates. The discrete element method (DEM) is the most commonly used discrete method, based on the finite difference discretization approach [17, 18]. DEM models the solid matrix of the reservoir formation with a packed particle assembly [25]. The particle assembly's mechanical behaviour is determined by the contact and bonding laws. If there is no change in contact and bonding states, the assembly behaves elastically. However, if some contacts start to separate or slip or bonding breakage occurs, the assembly begins to exhibit plastic behaviour. The detachment of an element or clump from the matrix is a natural consequence of losing its connections with other elements that are still associated with the solid matrix. Detached elements can also be trapped and reabsorbed by the solid matrix [27]. It is clear that DEM is a suitable approach for modelling the solid matrix component in sand production. A detailed description of the distinct element calculation algorithm is provided by Itasca (2008a). Figure 5 represents the DEM calculation cycle in each calculation cycle. The flow chart summarises the DEM calculation sequence, with each calculation cycle representing a computational time step. Once the geometry is defined, the calculation is performed for a specified number of cycles. At the start of each time step, contact forces are calculated based on the overlap between particles or between particles and walls, using the contact constitutive model. The resultant force on each particle is then determined by summing the contact and externally applied forces. Particle acceleration is determined by applying Newton's second law of motion. Finally, integration is used to calculate the incremental velocity and displacement of each particle. Prior to the next calculation cycle, the positions of all particles are updated to ensure accurate calculations.

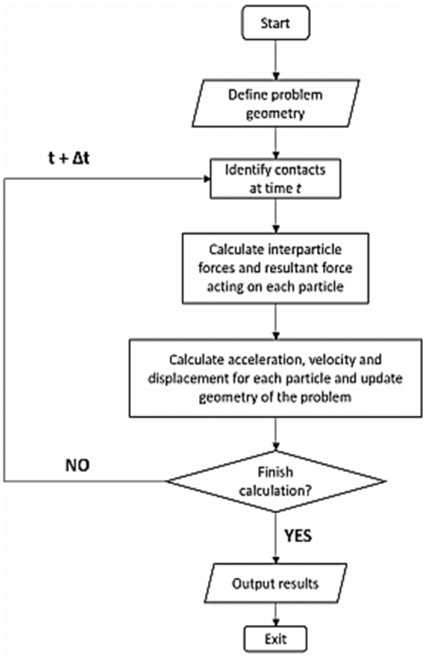

Figure 5. Flowchart for calculating DEM [30].

Several research studies have attempted to use DEM for simulating solid-fluid interactions. In a study by Tsuji (1993), a solid-fluid couple was developed. The fluid phase was discretized into elements larger than the particle sizes, and the average values of the pore pressure and fluid velocity were calculated within each grid block. The fluid phase was discretized into elements larger than the particle sizes, and the average values of the pore pressure and fluid velocity were calculated within each grid block. The fluid force was then calculated in each block, and applied to each discrete particle. Clean (1993) used the finite difference method to solve the fluid flow equations and coupled the continuum fluid flow problem with DEM solids [39]. In a two-dimensional model, [8] investigated the fluid pressure gradient behind solid particles using the discrete component method. The research was presented by examining the control volume to determine fluid speed in a two-dimensional direction. The flow rate was also determined by extrapolating the velocities to the force. The study investigated sand production under isotropic or non-isotropic stresses applied to the wall, as well as the application of separate

boundary pressures in addition to the applied stresses. The research indicates that sand production increases in non-isotropic conditions and with higher boundary pressure [16, 37]. A PFC software model was used to investigate this process by passing gas fluid flow. The amount of sand production increases with an increase in fluid pressure gradient behind the particles and tension around the well [37]. In 2018, a two-dimensional model was presented using the PFC 2D software to discuss the role of fluid flow in sand production. The research found that the fluid flow rate increases with a higher pressure gradient, leading to the separation of solid particles and an increase in sand production speed [36]. This study presents the verification of a numerical model against analytical solutions. The verified model is then used to simulate sanding for a synthetic laboratory scale problem. The effects of boundary stresses and fluid flow on sandstone degradation and sand production are analyzed. The particle flow code (PFC) developed by Itasca for the DEM calculations is adopted. In PFC, particles are typically considered rigid, but small overlaps are permitted at the contact points based on the stiffness of each particle. These overlaps are similar to the deformations that occur at real particle contacts in geo-materials. The contact between two adjacent particles is non-existent if there is no overlap between them.

3. Materials and Methods

The research work employs a device that simulates the flow of different fluids under varying stresses through rocks or sand particles to predict sand production in an oil well. The device comprises a cubic steel chamber measuring 15 x 15 x 10 cm, hydraulic jacks, a fluid injection pump (up to 4 bar), a 40-liter fluid tank, pressure gauges, control valves, and a computer scale. The device is built to a scale of 1/10. The device's production pipe has a diameter of 3 cm, equivalent to a well with a diameter of 30 cm [see Figure 6]. It is important to note that the production tube is replaceable and can be used with different perforations. The device operates by pouring dry sand into the chamber and placing a steel plate (piston) inside. The hydraulic jack is then placed on the steel plate and closed. This hydraulic jack can apply pressure up to 600 bar. Once the sand in the chamber is saturated, the fluid flows into the wall tube along with the sand. The production rate of sand and fluid in different states can be measured by calculating the weight of the fluid and sand and the time of the test.

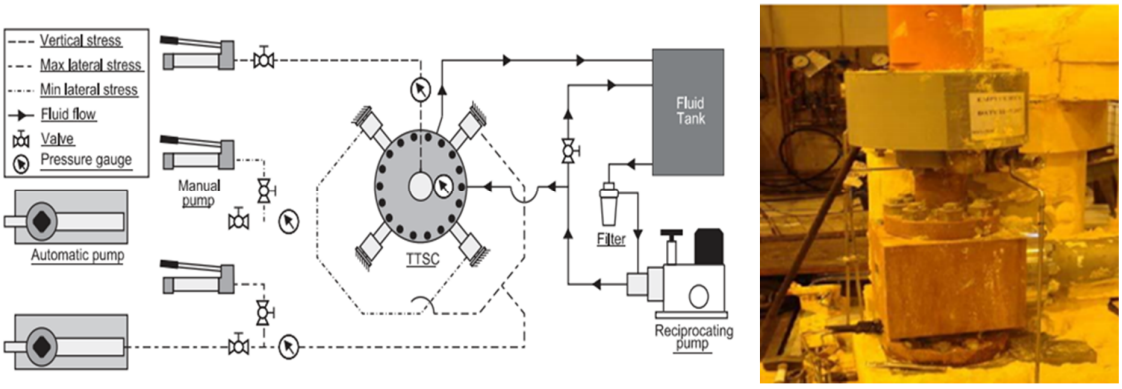

Figure 6. Sand production test device based on applying lateral stresses [28].

Two samples, C and B, were prepared according to the characteristics outlined in Table 1 [Figure 7]. In this laboratory section, we studied over 30 different articles, and selected two samples to investigate the different modes of low resistance to high resistance in sand production. The first sample has less resistance, while the second sample has more resistance. Tests were performed separately for each sample at 1, 5, 10, and 15 minutes. Table 2 presents the laboratory test results for both samples.

Figure 7. Laboratory environment.

Table 1. Laboratory characteristics of prepared samples.

Porosity	Poisson's ratio	Young modulus (Gpa)	Resistance (MPa)	Density (g/cm^3)	Hardness	Type of material	Sample
0.36	0.18	1.8	4.9	1.74	6	Sand	B
0.28	0.19	2.3	7.5	1.92	-	Fine sand	C

Figure 8 shows the samples after the test. Comparison charts were checked for each sample and all four modes. In the first case, the lateral stress was 25 MPa and the fluid pressure was 2 MPa, as shown in Figure 9 (a). The two samples have grown almost identically, with little difference between them, the sample C, which has a lower production rate, exhibited greater resistance. In the next state, as seen in Figure 9 (b), the stress value remained constant at 25 MPa, but the fluid pressure increased to 3 MPa. Figure 9 (c) shows that the changes in both samples were slightly different compared to the first case. Sample C shows more changes. Figure 9 (d) shows that sand production is initially lower when lateral stresses increase, but as stress surpasses particle forces, sand production increases. When two parameters increase together, sandblasting starts at a lower level than in previous cases, but failure occurs strongly once fluid forces overcome the particles.

Table 2. The modified TWC tests for sand production in laboratory.

Sand production sample C (gram)	Sand production sample B (gram)	Time (min)	Condition (MPa)	
150	180	1	**Stress = 25 Fluid pressure = 2**	**Test 1**
254	290	5		
310	380	10		
328	390	15		
195	190	1	**Stress = 25 Fluid pressure = 3**	**Test 2**
308	310	5		
320	330	10		
400	420	15		
270	280	1	**Stress = 35 Fluid pressure = 2**	**Test 3**
310	300	5		
315	310	10		
415	400	15		
120	140	1	**Stress = 45 Fluid pressure = 4**	**Test 4**
250	230	5		
554	610	10		
410	490	15		

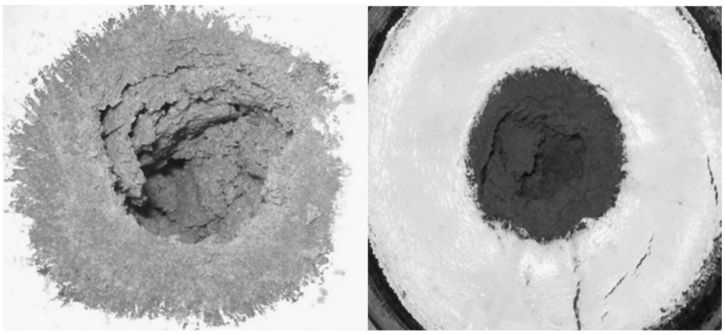

Figure 8. A section of two sandstone samples after the TWC test.

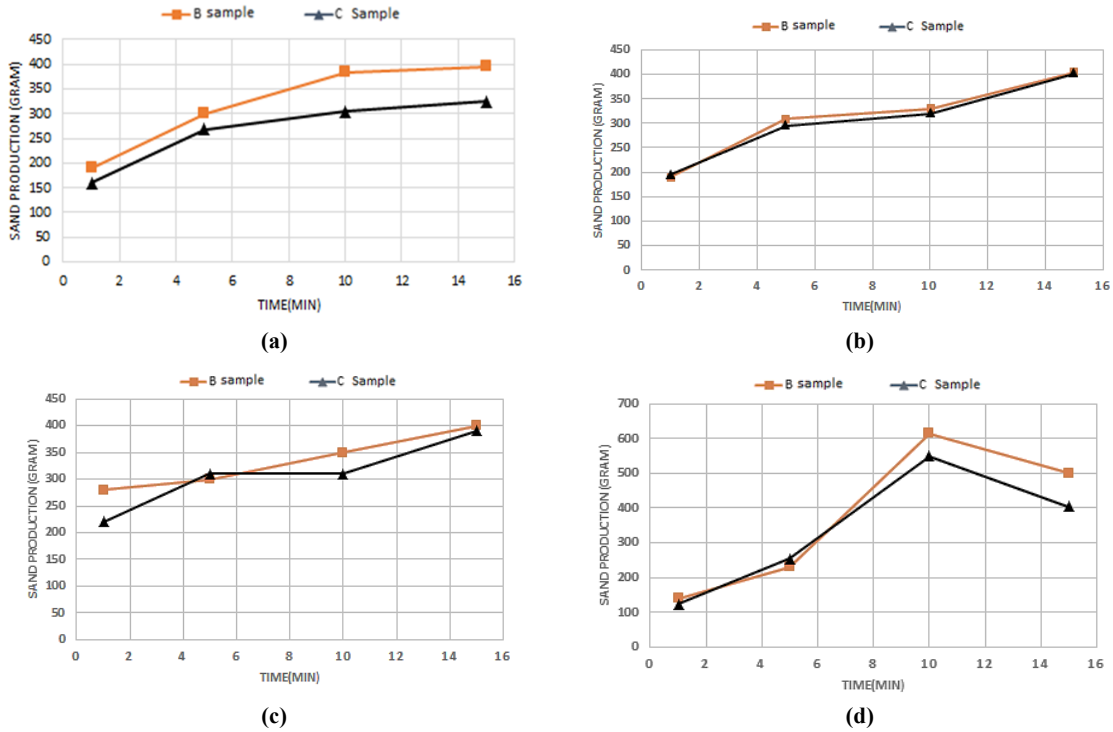

Figure 9. Comparison of sand production rate for two samples B and C: (a) stress = 25 MPa, fluid pressure = 2 MPa; (b) stress = 25 MPa, fluid pressure = 3 MPa; (c) stress = 35 MPa, fluid pressure = 2 MPa; (d) stress = 45 MPa, fluid pressure = 4 MPa.

4. Numerical Modeling

When modelling particles and materials, the most suitable method is the discrete element method, and it is best to use the PFC software. Modelling any type of test using PFC2D software involves two general coding parts. The first part involves creating a sample with suitable specifications such as compression, porosity, and desired geometry with standard dimensions [Figure 10]. The second part involves uploading the sample. The standard process for creating samples for rock modelling includes five steps:

i) The first step involves compressing the granular particles. This is done by creating walls using several flat and frictionless plates. Next, a set of particles with the desired distribution is produced to fill the container. The number of particles in the initial compaction is determined to create the desired initial porosity of the model in the particle assembly container. The particles are randomly placed in the environment with a maximum radius equal to half the desired radius to prevent overlap. The particle radius is then increased to achieve the desired porosity for the modeled assembly.

ii) To establish isotropic stress in the particle assembly, the radius of all particles within the container is reduced. The isotropic stress condition is obtained by calculating the average direct stress, which is the result of dividing the total force on the walls by the cross section of the modeled sample.

iii) To achieve a robust geomaterial model, it is recommended to omit or reduce the number of suspended (unbounded) particles in the particle assembly.

iv) Creating appropriate parallel bands between the particles in the assembly. These parallel bonds are created in the form of a regular network in all particles that are adjacent to each other. This proximity is realized when the distance between the surfaces is less than 10 times the average radius of the two particles.

v) The production process involves removing the floating particles and walls from the periphery of the model. The production process involves removing the floating particles and walls from the periphery of the model. This allows the model to behave freely and reach equilibrium.

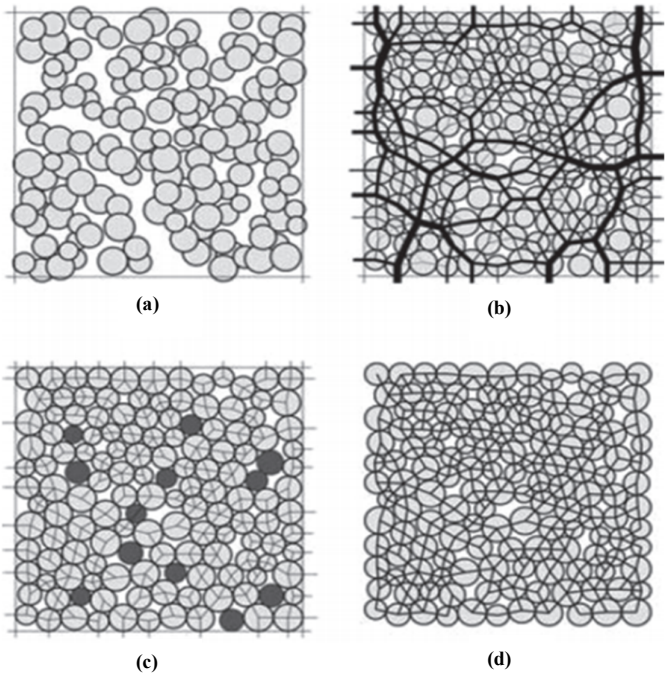

Figure 10. Model building steps in the software: (a) particle assembly after initial generation but before rearrangement; (b) contact force distribution after the second step; (c) floating particles and contacts after the second step; and (d) parallel-bond network [41].

Prior to conducting numerical modelling and verifying the mechanism, it is essential to create an artificial rock sample and calibrate the numerical model using the laboratory artificial rock. This ensures that the macro-mechanical behaviour of the numerical model of the artificial rock such as uniaxial, triaxial, and Brazilian resistance aligns with the mechanical behaviour of the virgin rock. The modelling is performed in two dimensions using the Particle Flow Code (PFC2D). Calibration was performed using laboratory test results for the uniaxial compressive strength of two artificial sandstone rocks.

3.1. Calibration of geomaterial model

Numerical modelling using the FLAC and UDEC software requires the direct extraction of macro-mechanical characteristics such as Young's modulus, Poisson's ratio, and uniaxial resistance, from laboratory results and their application to the model.

In PFC, it is not possible to directly apply macro-mechanical properties to the model. Instead, the ideal macro-mechanical properties of the model should be estimated by selecting appropriate micro-mechanical properties such as normal and shear stiffness of connections and Young's modulus of connections. This will ensure that the numerical and laboratory macro-mechanical behavior is similar. The two samples selected for calibration are from Natalia Pera's work (Natalia Pera, 2016). The single-axis machine contains the same two samples, B and C, used in the laboratory stage. Table 3 provides the specifications and features of these samples. The particle type is disk-shaped, with a diameter ratio greater than 1 between the largest and smallest grains. If the grain dimensions are equal (ratio = 1), the behavior will

be isotropic, which differs from the natural behavior of rock grains. For this analysis, dimensions of 0.6 and 0.7 were chosen to reflect static conditions.

Table 3. Micro- Parameters for calibration.

Sample C	Sample B	Micro-parameters
Disc	Disc	Particle type
1.92	1.74	Density (g/cm^3)
0.2	0.2	Minimum disk radius
0.7	0.6	damping coefficient
15	13.8	Young's modulus of contact (Gpa)
3.6	2.9	Hardness ratio of contact connection
15	13.8	Young's modulus of parallel connection (Gpa)
3.6	2.9	Parallel connection stiffness ratio
0.4	0.4	friction coefficient
29	31.5	Normal resistance of parallel connection (MPa)
29	31.5	Shear strength of parallel connection (MPa)
14.5	15	Parallel bond adhesion (MPa)

For the uniaxial compression test simulation, we used a model depicted in Figure 11. The model has a height of 110 mm and a width of 50 mm, and both samples have the same dimensions. The loading is simulated by two moving plates that apply pressure to the set of disks.

Figure 12 (a) displays the stress-strain diagram obtained from the numerical simulation of sandstone B and the fracture pattern of the numerical model. In (b), the stress-strain diagram obtained from the numerical simulation for sample C is shown. The results of the uniaxial compressive strength test in this research work are in acceptable agreement with the numerical and laboratory results of two sandstone samples, as shown in Table 4. This table will be used for further discussions and modelling in the software.

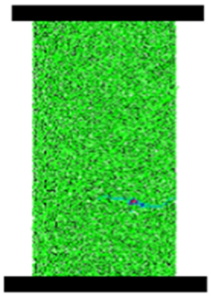

Figure 11. Model built under uniaxial test, height of 110 mm, and a width of 50 mm.

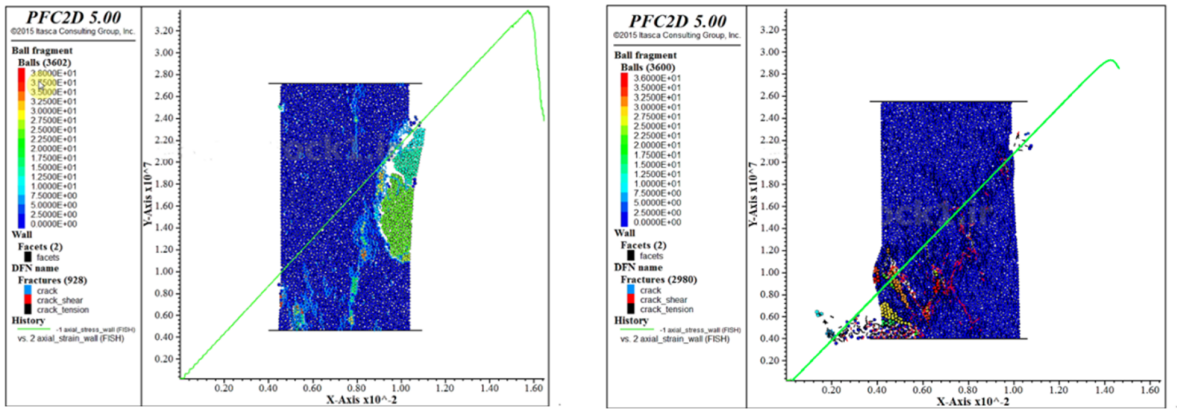

(a) **(b)**

Figure 12. Stress-strain diagram obtained from numerical modeling of: (a) sample B, (b) sample C.

Table 4. Macro-mechanical parameters for calibration in PFC2D.

Young's modulus (Gpa)	Poisson's ratio	Uniaxial compressive strength (MPa)	The results of the samples as:	
8.5	-	33	Laboratory (Natalia pera, 2016)	Sample B
8.5	0.18	31.8	Numerical modeling of this article (Natalia pera, 2016)	
7	0.15	36	Numerical modeling in this research work	
6	-	28	Laboratory (Natalia pera, 2016)	Sample C
6.5	0.19	26.5	Numerical modeling of this article (Natalia pera, 2016)	
4.5	0.15	32	Numerical modeling in this research work	

3.2. Validation

The accuracy of the numerical modelling results obtained from PFC2D should be validated by model fitting with the laboratory test results. In this study, the fluid pressure parameters are compared with the laboratory results of Natalia in 2016 (Natalia Pera, 2016) and the simulation results of [16]. The calibration results of Sandstone B are used for validation. To simulate the production of sand, a sample with dimensions of 15 x 15 cm and a hole with a diameter of 3 cm containing disc particles with a radius of 0.2 to 0.3 mm, was built using the data from Table 1. Figure 13 shows the example constructed.

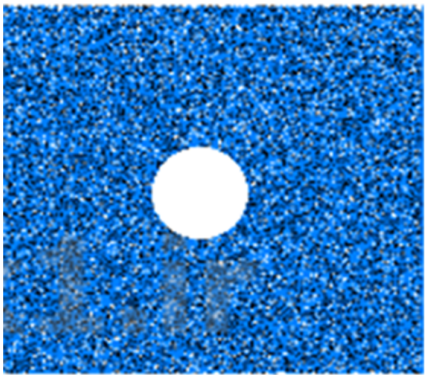

Figure 13. Model made in PFC2d.

Figure 14 (a) shows the simulation results in pfc2d software and (b) Yifie results in 2016 for the case where the fluid pressure is 10 MPa. The way in which the particles are separated and emptied around the wall is in good agreement with the 2016 Yifie results. Figure 14 (c) shows the simulation results in pfc2d software and (d) Yifie results in 2016 for the case where the fluid pressure is 25 MPa. The uniaxial test modelling results in this study is in relatively good agreement with the uniaxial compressive strength results of Sandstone B, and there is a difference of about 10%. Also the simulation results in PFC2D software and Yifie results in 2016 showed that PFC2D software is reliable and accurate enough to model sand production mechanisms.

5. Numerical Modeling of Modified laboratory TWC Tests

This section compares the laboratory test data of sand production for two sandstone samples, B and C, by creating models in the software, and comparing the results obtained with the modeling results. To simulate sand production, a sample with dimensions of 15 x 15 cm and a 3 cm diameter hole was used, based on the data from Table 1. Figure13 illustrates the example that was built.

In the first case, Figure 15 (a) shows the results of sand production modelling for two samples, B and C, with constant stress and fluid pressure, and lateral stress equal to 25 MPa and fluid pressure equal to 2 MPa. The laboratory and modelling results are almost identical. Figure 15 (b) shows a constant stress value of 25 MPa and a fluid pressure of 3. In this case, the results for both samples are more compatible. Figure 15 (c) shows a constant fluid pressure of 2 MPa and a stress value of 35, except for the beginning of the sand production stage in the sample. The laboratory and modeling results are presented. results are almost equal. In the last case, when the two parameters stress and fluid pressure increase together, the At a stress level of 45 and fluid pressure of 4 MPa, sand production reaches its peak and subsequently decreases over time, as shown in Figure 15 (d), which presents the laboratory and numerical modeling results.

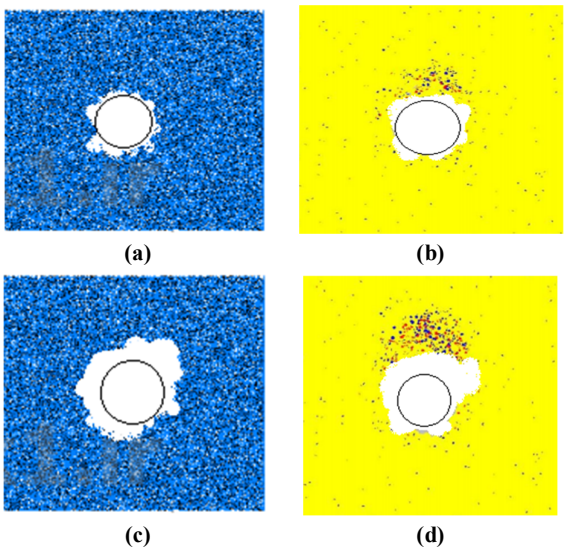

Figure 14. Comparison of the simulated models with the Yifie's models: (a) Simulation results with fluid pressure of 10 MPa; (b) Yifie results [16] at a fluid pressure of 10 MPa; (c) Simulation results at a fluid pressure of 25 MPa; (d) Yifie results [16] at a fluid pressure of 25 MPa.

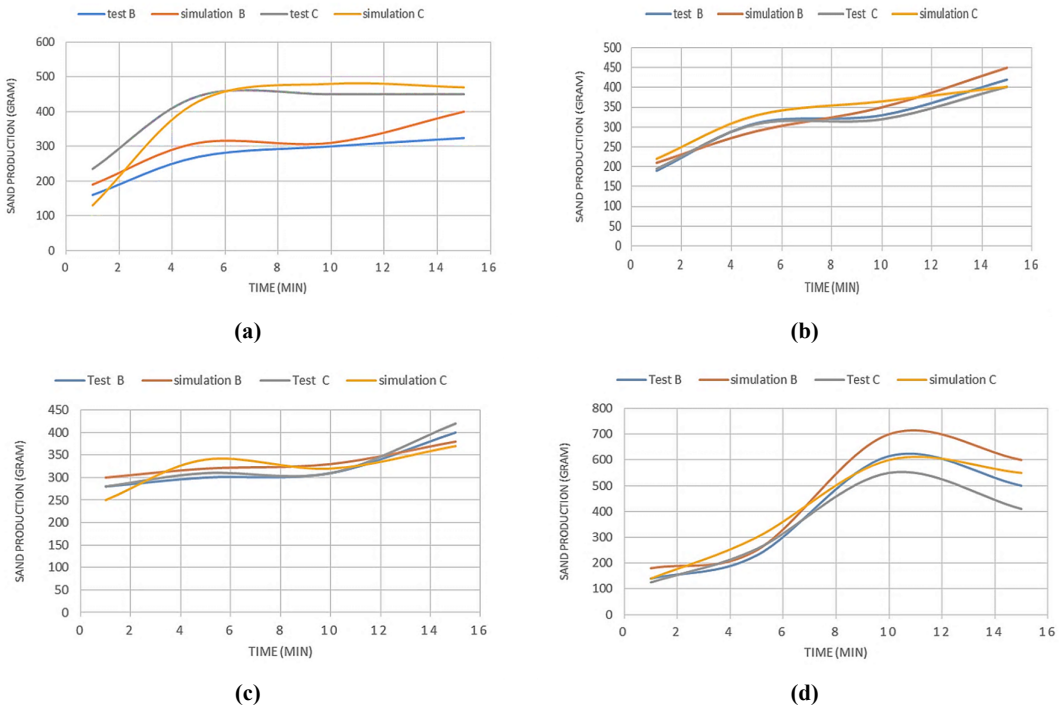

Figure 15. Comparison of simulation results with laboratory results for two samples B and C: (a) stress = 25 MPa, fluid pressure = 2 MPa; (b) stress = 25 MPa, fluid pressure = 3 MPa; (c) stress = 35 MPa, fluid pressure = 2 MPa; (d) stress = 45 MPa, fluid pressure = 4 MPa.

Generally, sand production increases with higher fluid pressure and lateral stress in both samples. Figure16 compares physical data and numerical modeling of fluid pressure changes and sand production for sample B and sample C, respectively, as fluid pressure increases while stress remains constant. For Sample B, an increase in fluid pressure results in a faster sand production rate compared to Sample C due to its lower resistance. The laboratory tests and modeling results for both samples under changing fluid pressure and tension demonstrate acceptable compliance.

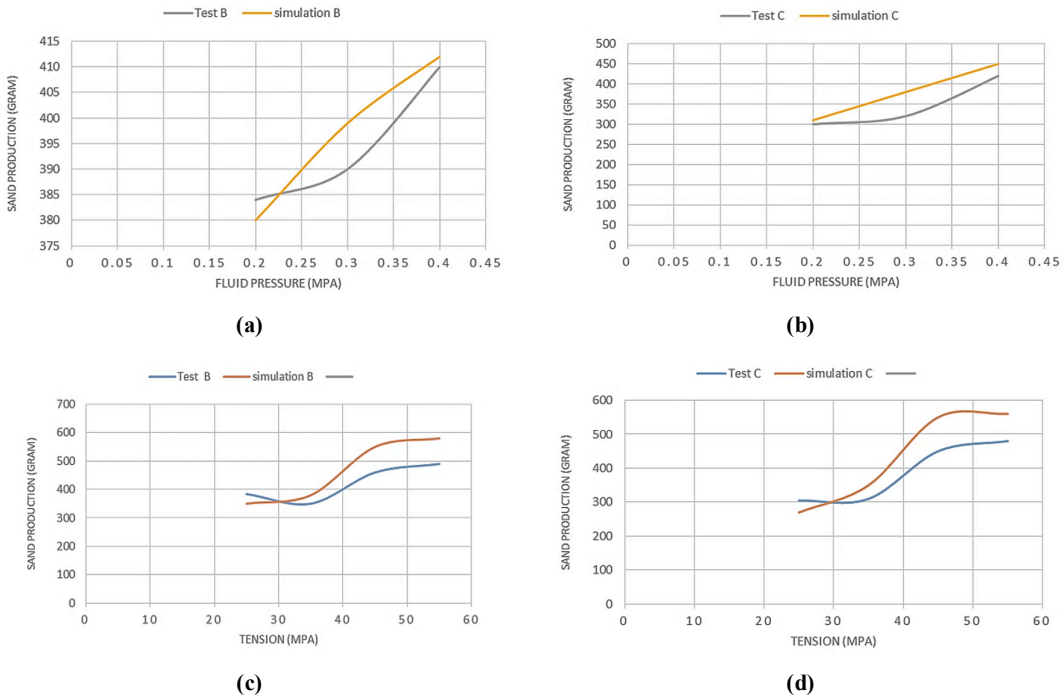

Figure 17. Comparison of simulation results with laboratory results: (a) sample B, variable fluid pressure; (b) sample C, variable fluid pressure; (c) sample B, variable stress; (d) sample C, variable stress.

6. Conclusions

This work examines sand production as a problem during the production stage of a wellbore. The sand production mechanism is influenced by two main factors: effective stress and fluid pressure applied to the particles. Therefore, the process of sand production in oil wells has emphasized these two parameters. Laboratory tests on sandstone specimens have been modified by changing each parameter, and the sand production rate has been measured. The same tests have been numerically modeled with PFC2D, and the computed results have been compared with the corresponding measured values obtained from the experimental tests. The following conclusions have been drawn:

1. Higher pressure of fluid causes earlier destruction of the sandstone samples and after this destruction; stress reduction on the model is observed leading to the enhancement of sand production. It means that as the effective stress decreases the rate of sand production increases.
2. When the lateral stresses increased, the sand production is reduced but as soon as the amount of stress overcomes the forces between the particles, sand production increases dramatically.
3. There is a reasonable process of sand production in the modified WTC tests because a suitable correlation between variables is provided.
4. The laboratory device has a suitable repeatability, so the device can be used to predict and model sand production in oil wells.
5. The numerical simulation of the modified TWC tests provides the opportunity to consider the mechanism of sand production in different rock reservoirs under harsh environmental conditions.
6. In general, with increasing fluid pressure and increasing lateral stress in both samples, an increase in sand production is evident both from the measured laboratory results and from the numerical modeling results obtained by PFC2D.

In the future of sand production processes, one potential area of discussion is the modelling of the complex failure mechanism around the well bore. Further achievements can be gained from fracture mechanics analyses of oil wells during the production stage of the reservoir, as many cracks and micro-cracks may produce and propagate around the well wall.

References

[1] Dusseault MB and Santarelli FJ A. (1989). Conceptual model for massive solids production in

poorly-consolidated sandstones. *Rock at great depth. 2(1),*789–797.

[2] Fjaer. E, Holt RM, Horsrud P, Raaen AM, and Risnes R. (1992) Petroleum related rock mechanics. Amsterdam.

[3] Bianco LC. (1999) Phenomena of sand production in non-consolidated sandstones. PhD thesis. Penn State University, University Park, Penn.

[4] Toma P, Harris B, Korpany G, Bohun D, and George A. (2009). Experimental investigations for reducing the risk of sand inflow in slotted horizontal wells. *Proceedings of the ASME energy source technical conference and exhibition. 23(5)*: 1–10.

[5] Geilikman MB and Dusseault MB. (1997). Dynamics of wormholes and enhancement of fluid production. *Proceedings of the 48th annual technical meeting of the petroleum society*. 8–11.

[6] Unander TE, Papamichos E, Trovoll J, and Skjaerstein A. (1997). Flow geometry effects on sand production from an oil producing perforation cavity. *J Rock Mech Min. 34(3)*: 1–15.

[7] A. Nouri, E. K. (2009). Elastoplastic modelling of sand production using fracture energy regularization method. *Journal of Canadian Petroleum Technology. 48(4)*: 64–71.

[8] A. Ghassemi, A. (2015). Numerical simulation of sand production using a coupled lattice Boltzmann-DEM, *Journal of Petroleum Science and Engineering*. *54(1)*: 218-231.

[9] A. Hauwa Christiana, A. (2015). Sand control using geomechanical techniques: a case study of Niger delta, Nigeria, *Journal of science inventions today. 5(1)*: 439-450.

[10] A. lues, E. L. R. C. (2011). Numerical analysis of sand/solids production in boreholes consideringfluid mechanical coupling in a Cosserat continuum. *International Journal of Rock Mechanics & Mining Sciences. 48(8)*: 1303-1312.

[11] A. Zervos, P. P. (2001). Modelling of localisation and scale effect in thick-walled cylinders with gradient elastoplasticity. *International Journal of Solids and Structures. 38(30)*: 5081–5095.

[12] A. Zervos, P. P. (a-2001). A finite element displacement formulation for gradient elastoplasticity. *International Journal for Numerical Methods in Engineering. 50(6)*: 1369–1388.

[13] A. Yuonessi, V. B. (2013). Sand production simulation under true - triaxial stress conditions. *International Journal of Rock Mechanics and mining Science. 61*: 130-140.

[14] Asgian, M. P. (1995). Mechanical stability of propped hydraulic fractures: A numerical study. *Journal of Petroleum Technology. 47(3)*: 203-208.

[15] Bradley, H. (1987). Society of Petroleum Engineers. *In Petroleum Engineering Hand Book*.

[16] Bratli, R. A. (1981).Stability and failure of sand arches. *SPEJ*, 236-248.

[16] C. Yufi, A. E. (2016). A new approach to dem simulation of sand production. *Journal of Petroleum Science and Engineering. 147*: 56-67.

[17] Cook BK, Lee MY, Digiovanni AA, Bronowski DR, Perkins ED, and Williams JR. (2004). Discrete element modeling applied to laboratory simulation of near-wellbore mechanics. *Int J Geomech. 4*: 9–27.

[18] Li L, Papamichos E and Cerasi P. A study of mechanisms of sand production using DEM with fluid flow. In: Cotthem AV, editor. *Proceedings of the Eurock 06*.

[19] Ehsan Khamehchi, E. R. (2015). Sand production prediction using ratio of shear modulus to bulk compressibility (case study), Egyptian. *Journal of Petroleum. 24(2)*: 113-118.

[20] Farhad Gharagheizi, A. M. M. (2016). Prediction of sand production onset in petroleum reservoirs using a reliable classification approach. *Petroleum. 3(2)*: 1-6.

[21] Sanei M, Duran O, and Devloo PRB. (2017). Finite element modeling of a non-linear poromechanic deformation in porous media. *In Proceedings of the XXXVIII Iberian Latin American Congress on Computational Methods in Engineering*. 10.20906/CPS/CILAMCE2017-0418.

[22] Duran O, Sanei M, Devloo PRB, and Santos ESR. (2020). An enhanced sequential fully implicit scheme for reservoir geomechanics. *Comput Geosci 24(4)*:1557–1587.

[23] Sanei M, Durán O, Devloo PRB, and Santos ESR. (2021). Analysis of pore collapse and shear-enhanced compaction in hydrocarbon reservoirs using coupled poro-elastoplasticity and permeability. *Arab J Geosci. 14(7).*

[24] Sanei M, Durán O, Devloo PRB, and Santos ESR (2022) Evaluation of the impact of strain-dependent permeability on reservoir productivity using iterative coupled reservoir geomechanical modeling. *Geomech Geophy Geo Energy Geo Res. 54(2).*

[25] Abdollahipour A, Kargar A , and Fatehi Marji M. (2023). Numerical modeling of the effect of Anderson's stress regimes on the volume of sand production in oil wellbores. *Journal of Analytical and Numerical Methods in Mining Engineering. 13(35)*: 31-38.

[26] Abdollahipour A and Fatehi Marji M.(2023). Numerical modeling of borehole breakouts formation in various stress fields using a Higher-Order Displacement Discontinuity Method (HODDM). *JOURNAL OF PETROLEUM GEOMECHANICS. 4(3)*: 1-18.

[27] Yousefian H, Soltanian H, Fatehi Marji M, Abdollahipour A, and Pourmazaheri Y. (2018).

Numerical simulation of a wellbore stability in an Iranian oilfield utilizing core data. *Journal of Petroleum Science and Engineering. 168*: 577-592.

[28] H. Rahmati, A. N. (2011). Validation of predicted cumulative sand and sand rate against physical-model test. *Journal of Canadian Petroleum Technology. 51(5)*: 403–410.

[29] Hossein Rahmati, M. J. (2013). Review of Sand Production Prediction Models. *Journal of Petroleum Engineering.*

[30] Ispas, I. R. (2002). Prediction and evaluation of sanding and casing deformation in a GOM shelf well. *Proceedings of SPE/ISRM Rock Mechanics Conference*. Irving‹Texas‹USA.

[31] Natalia Climent Pera (2016). A Coupled CFD-DEM Model for Sand Production in Oil Wells. Ph.D. thesis, Barcelona, September 2016.

[32] Siavash Ashoori, M. M. (2014). Prediction of critical flow rate for preventing sand production using the mogi-coulomb failure criterion, *Sci.Int (Lahore). 26(5)*: 2029-2032.

[33] Taghilou M and Rahimian MH. (2015). Simulation of 2D droplet penetration in porous media using lattice Boltzmann method. *Modares Mech Eng. 3*: 43-56.

[34] Z. M. Zhu, W. T. Xu, and R. Q. Feng. (2015). A new method for measuring mode-I dynamic fracture toughness of rock under blasting loads. *Experimental Techniques.*112

[35] Gago, P.A., Raeini, A.Q., and King, P. (2020). A spatially resolved fluid-solid interaction model for dense granular packs/soft-sand. *Adv. Water Resour. 136*: 103454.

[36] Garolera, D., Carol, I., and Papanastasiou, P. (2019). Micro-mechanical analysis of sand production. *Int. J. Numer. Anal. Methods GeoMech. 43*: 1207-1229.

[37] Zheng, H., Pu, C., Wang, Y., and Sun, C. (2020). Experimental and Numerical Investigation on Influence of Pore-Pressure Distribution on Multi-Fractures. *Tight Sandstone Engineering Fracture Mechanics*, 106993.

[38] Speight, J.G. (2020). Petroleum and Oil Sand Exploration and Production Fossil Energy.17-45.

[39] Sun, S., Zhou, M., Lu, W., and Davarpanah, A. (2020). Application of symmetry law in numerical modeling of hydraulic fracturing by finite element method. *Symmetry.12 (7)*:11-22.

[40] Fattahpour V, Moosavi M, and Mehranpour M.(2012). An experimental investigation on the effect of rock strength and perforation size on sand production. *Journal of Petroleum Science and Engineering. (86-87)*: 172-189.

[41] Fattahpour V, Moosavi M, and Mehranpour M (2012). An experimental investigation on the effect of grain size on oil-well sand production. *Petroleum Science. (9)*: 343-353.

[42] Veeken, C., Davies, D., Kenter, C., and Kooijman, A. (1991). Sand production prediction review: Developing an integrated approach. 66th Annual *Technical Conference and Exhibition of the Society of Petroleum Engineers*. Dallis, US. SPE 22792.

[43] Al-Shaaibi, S.K., Al-Ajmi, A.M., and Al-Wahaibi, Y. (2013). Three-dimensional modeling for predicting sand production. *J. Pet. Sci. Eng.* 109: 348–363.

[44] Papamichos, E. (2006). Sand production: Physical and experimental evidence. *Special issue of Revue européenne de génie civil, 10(6-7)*: 803-816.

[45] Papamichos, E., Tronvoll, J., Skjaerstein, A., and Unander, T. E. (2010). Hole stability of Red Wildmoor sandstone under anisotropic stresses and sand production criterion. *Journal of Petroleum Science and Engineering. 72*: 78-92.

[46] Jinwei Fu, Haeri H, Sarfarazi V, Naderi A, Jahanmiri SH, Jafari J, and Fatehi Marji M.(2023). Failure mechanism of circlular tunnel supported by concrete layers under uniaxial compression: Numerical simulation and experimental test. *Journal of Theoretical and Applied Fracture Mechanics. 125*: 103839.

[47] Lei Zhou, Haeri H, Sarfarazi V, Abharian S, Khandelwal M, and Fatehi Marji M.(2023). Experimental test and PFC3D simulation of the effect of a hole on the tensile behavior of concrete: A comparative analysis of four different hole shapes. *Journal of Mechanics-based Design of Structures and Machines*. 1-23.

[48] Emami Meybodi E, Hussain SK, and Fatehi Marji M. (2023). Experimental Evaluation and Discrete Element Modeling of Shale Delamination Mechanism. *Journal of Mining and Environment*.

مدلسازی مکانیزم تولید ماسه در چاه نفت با در نظر گرفتن اثرات تنش درجا و فشار سیال با روش المان گسسته

مسعود یزدانی[۱]، محمد فاتحی مرجی[۱*]،حمید سلطانیان[۲]، مهدی نجفی[۱]و منوچهر صانعی[۱]

۱- گروه مهندسی معدن و متالورژی، دانشگاه یزد، یزد، ایران

۲- گروه تحقیقات و فناوری های حفاری و تکمیل چاه، پژوهشکده صنعت نفت، تهران، ایران

ارسال ۲۰۲۳/۱۱/۲۷، پذیرش ۲۰۲۴/۰۱/۲۲

* نویسنده مسئول مکاتبات: mohammad.fatehi@gmail.com

چکیده:

تقریباً ۷۰ درصد از میادین هیدروکربنی جهان در مخازنی با سنگ‌های کم استحکام مانند ماسه سنگ قرار دارد. در طول تولید هیدروکربن‌ها از مخازن ماسه سنگ، ذرات به اندازه ماسه ممکن است از سازند خارج شده و وارد جریان سیال هیدروکربنی شوند. تولید شن و ماسه به دلیل پتانسیل ایجاد فرسایش لوله‌ها و شیرها، موضوع مهمی در صنعت نفت است. جداسازی ذرات از نفت فرآیندی پرهزینه است، از این رو شرکت‌های تولید کننده نفت و گاز انگیزه دارند تا تولید شن و ماسه را در حین استخراج کاهش دهند. روش‌های مختلفی برای پیش‌بینی این پدیده وجود دارد که شامل روش‌های پیوسته، ناپیوسته، تجربی، فیزیکی، تحلیلی و عددی می‌شود. با توجه به اهمیت موضوع، این تحقیق با دستیابی به دو هدف اصلی انجام شده است. در مرحله اول، یک مدل عددی دو بعدی را بر اساس روش المان گسسته برای رسیدگی به مسائل کرنش و تغییر شکل زیاد در مواد دانه‌ای پیشنهاد می‌کند. این روش در شبیه سازی مکانیسم تولید شن و ماسه در چاه‌های نفت بسیار قابل اعتماد است. ثانیاً، تولید ماسه تحت تأثیر دو عامل فشار سیال و تنش است، که برای ارزیابی تغییرات تولید از یک مخزن خاص، لازم است هر پارامتر تجزیه و تحلیل شود. دو نمونه ماسه سنگ مشابه شرایط سنگ مخزن تهیه و در آزمایشگاه برای نشان دادن پدیده تولید ماسه مورد آزمایش قرار گرفت. نتایج عددی اعتبارسنجی و با همتایان تجربی خود مقایسه شده است.

کلمات کلیدی: روش المان گسسته؛ تولید ماسه؛ فشار سیال؛ چاه نفت؛ تست سیلندر دیواره ضخیم.